

# Meso Scale Model for Fiber-Reinforced-Concrete: Effective Bond-Slip Relationship of Fibers

---

**Smolčić, Željko; Ožbolt, Joško**

*Source / Izvornik:* **Zbornik radova Građevinskog fakulteta Sveučilišta u Rijeci, 2014, XVII, 197 - 212**

**Journal article, Published version**

**Rad u časopisu, Objavljena verzija rada (izdavačev PDF)**

*Permanent link / Trajna poveznica:* <https://um.nsk.hr/um:nbn:hr:157:679583>

*Rights / Prava:* [Attribution-NonCommercial-NoDerivatives 4.0 International/Imenovanje-Nekomercijalno-Bez prerada 4.0 međunarodna](#)

*Download date / Datum preuzimanja:* **2024-11-26**



image not found or type unknown

*Repository / Repozitorij:*

[Repository of the University of Rijeka, Faculty of Civil Engineering - FCERI Repository](#)



image not found or type unknown

GRAĐEVINSKI FAKULTET  
SVEUČILIŠTA U RIJECI



# Zbornik radova

XVII

Rijeka, 2014.

# MESO SCALE MODEL FOR FIBER-REINFORCED- CONCRETE: EFFECTIVE BOND-SLIP RELATIONSHIP OF FIBERS

## MEZO MODEL BETONA ARMIRANOG VLAKNIMA: EFEKTIVNA POSMIČNA VEZA IZMEĐU VLAKNA I BETONA

Željko Smolčić \*, Joško Ožbolt \*\*

### Sažetak

*U radu je prikazana eksperimentalna i numerička analiza betona armiranog čeličnim vlaknima s kukama. Eksperimentalna analiza provedena je savijanjem zarezanih greda u tri točke s različitim volumnim udjelima vlakana do 1,5%. Numerička analiza betona armiranog vlaknima provedena je na mezo nivou. Beton je modeliran s 3D solid konačnim elementima, dok je kao konstitutivni zakon korišten mikroravninski model. Vlakna su modelirana slučajno generiranim 1D štapnim konačnim elementima, a veza između betona i vlakana („interface“) modelirana je diskretnim bond elementima. Analiza realno odgovara eksperimentalnim rezultatima. U svim slučajevima, do otkazivanja dolazi zbog čupanja vlakana. Pokazano je da se porastom volumnog udjela vlakana smanjuje čvrstoća bonda i kapacitet prokliznuća vlakana.*

**Ključne riječi:** beton, čelična vlakna, analiza 3D konačnim elementima, mezo nivo, mikroravninski model, posmično naprezanja-prokliznuće

### Abstract

*The paper carries out an experimental and numerical analysis of hook-end steel fiber reinforced concrete. The experimental tests are performed on notched beams loaded in 3-point bending using fiber volume fractions up to 1.5 %. The numerical analysis of fiber reinforced concrete beams is performed at meso scale. The concrete is discretized with 3D solid finite elements and a microplane model is used as a constitutive law. The fibers are modelled by randomly generated 1D truss finite elements and the interface*

---

\* Faculty of Civil Engineering of University of Rijeka, Radmile Matejčić 3, Rijeka, Croatia  
E-mail: zeljko.smolcic@uniri.hr

\*\* Faculty of Civil Engineering of University of Rijeka, Radmile Matejčić 3, Rijeka, Croatia  
E-mail: drugi.ozbolt@iwb.uni-stuttgart.de

*between concrete and fibers is simulated by employing discrete bond-slip relationship. The analysis realistically replicates experimental results. In all investigated cases failure is due to the pull-out of fibers. It is shown that with increase of volume content of fibers the effective bond strength and slip capacity of fibers decreases.*

**Keywords:** Concrete, steel fibers, 3D finite element analysis, meso-scale, microplane model, bond-slip

## 1. Introduction

Fiber reinforced concrete is a composite material, to which, in addition to the usual concrete ingredients, small discontinuous fibers of high tensile strength are added during the mixing process. The fibers used in fiber reinforced concrete are classified according to the material they are made of: steel fibers, glass fibers, synthetic fibers and natural fibers [1]. Compared to the same concrete composition without fibers, fiber reinforced concrete has principally a higher compressive and tensile strength and fracture energy. The main advantages of fiber reinforced concrete are visible at the post peak response when the fibers bridge the cracks and contribute to the resistance and ductility [1].

Due to its composition, concrete is an extremely heterogeneous quasi-brittle material, not simple to model realistically. Addition of fibers to concrete increases its heterogeneity. From the numerical point of view, this makes the modelling even more complex. In the numerical modelling macro scale models are mostly used in engineering practice; however, numerically more demanding meso scale models provide better insight into the actual concrete behavior. Numerical studies are essential to improve the properties of the material, such as concrete or fiber reinforced concrete. Having a realistic numerical model, numerical parametric studies together with experiments can serve as important tool to improve material and structural properties. An overview of the models for modelling of fiber reinforced concrete is given in [2], according to which the majority of fiber reinforced concrete models are based on: (1) Models formulated in the framework of continuum mechanics using stress-strain ( $\sigma$ - $\epsilon$ ) relationship and smeared crack approach [3, 4]; (2) Discrete models based on the stress-crack opening law ( $\sigma$ - $w$ , discrete cracks) [5, 6] and (3) The combination of (1) and (2). The analysis can be carried out at the macro or meso scale.

For modelling at macro scale material properties must be homogenized and, depending whether the cracking is modelled using smeared or discrete approach, stress-strain softening law or stress-crack opening law is employed. However, when modelling at the meso scale, the fiber reinforced concrete is usually considered as a three - phase material consisting of:

cement matrix (concrete), fibers and interface between cement matrix and fibers. Every single fiber has to be modelled separately so that the fiber position and its orientation, as random variables, have to be determined. Typical examples of such modelling approach are based on the Lattice models and the Rigid-Body-Spring Model (RBSM) [2, 7, 8, 9, 10, 11].

In this paper experimental and numerical results of 3-point bending pre-notched beams made of fiber reinforced concrete are presented and discussed. In order to provide better insight into the actual behavior of fiber reinforced concrete, the numerical analysis is performed at the meso scale. The aim is to formulate the effective bond-slip relationship between fibers and concrete for different volume content of fibers. In the analysis fiber reinforced concrete is considered as a three-phase composite consisting of concrete, fibers and the interface between them. Concrete is discretized by 3D finite elements. The microplane model is used as a constitutive law. The fibers are modelled as simple truss finite elements that are randomly distributed over the concrete and represented by the uniaxial stress-strain relationship for steel. The connection between concrete and fibers is modelled with discrete bond-slip relationship. The calibration of parameters for concrete and for bond-slip relationship is obtained by fitting experimental results of concrete beams without and with different fiber content. Finally, numerical parametric study is carried out to formulate the relationship between volume content of fibers and bond-slip relationship.

## 2. Experimental investigations

Three-point bending tests are performed on pre-notched fiber reinforced concrete beams. In the experiments, the concrete quality is kept constant and only the volume content of steel fibers is varied in the range from 0 to 1.5 %. The experimental results are then used to calibrate the numerical model in order to formulate the relationship between volume content of fibers and effective bond-slip constitutive law for fibers.

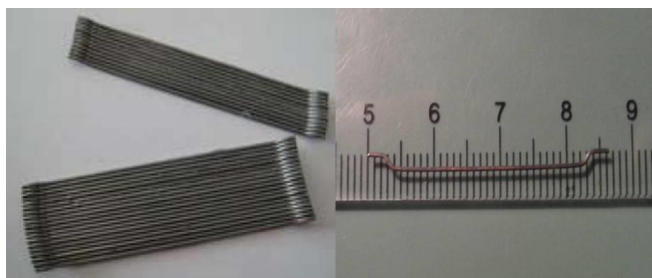
### 2.1. Material properties

The compressive and tensile strength of plain concrete are measured for three different concrete mixtures. The compressive tests are performed according to EN 12390-3 [12] standard on 150x150x150 mm concrete cubes. Three specimens of each mixture are tested, 9 specimens in total. The results (mean values) are shown in Table 1. Tensile splitting strength of concrete is measured according to EN-12390-6 [13] standard on 150x150x150 mm concrete cubes. The same as for compression, three specimens of each mixture are made and the results are summarized Table 1.

**Table 1.** Compressive and tensile strengths (mean values)

| Mixture | Compressive strength $f_c$<br>[MPa] | Splitting tensile strength $f_{ts}$<br>[MPa] |
|---------|-------------------------------------|--|
| M1      | 60.94                               | 3.96   |
| M2      | 74.47                               | 4.38   |
| M3      | 71.88                               | 4.20   |

In the fiber reinforced concrete the hooked-end steel fibers Dramix RC 65/35 BN are used. The fiber length being  $l_f = 35$  mm, the diameter  $d_f = 0.55$  mm (Fig. 1) and the aspect ratio  $l_f/d_f = 65$ . The fiber tensile strength is  $f_s = 1.345$  GPa and Young's modulus  $E_s = 210$  GPa.

**Figure 1.** Hooked-end steel fibers Dramix RC 65/35 BN

The objective of the study is to obtain the parameters needed for discrete modelling of bond between concrete and fibers. To obtain bond-slip relation for a single fiber, pull-out tests for single fiber are carried out on 40x40x160 mm concrete prisms for three different concrete mixtures. Three specimens of each mixture were made, in total 9 specimens were tested. The steel fibers were embedded in the middle of the concrete prism, with the embedment length equal to one fourth of the fiber length ( $l_e = l_f/4 = 35/4 \approx 9$  mm). The axis of the fiber is perpendicular to the surface of the concrete specimen. The pull-out tests are carried out by displacement control, the constant displacement rate being 0.005 mm/s. The experiment is conducted until the fiber is completely pulled out of the specimen (total displacement of 9 mm). The measured pull-out load vs. fiber displacement curves and the corresponding mean value curve are shown in Fig. 2.

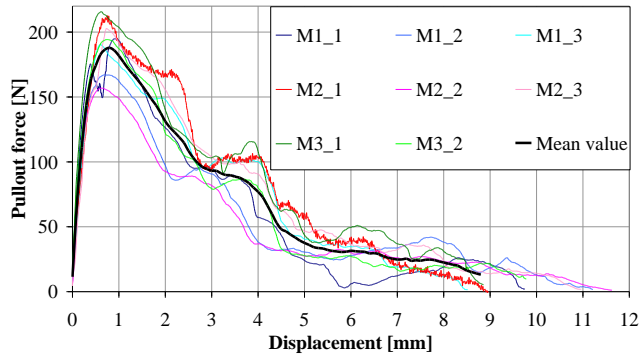


Figure 2. Single fiber pull-out force vs. slip curves

### 2.2. Three-point bending tests on pre-notched beams

The bending tests are carried out on square cross-section beams  $b \times h = 150 \times 150$  mm of the total length  $L = 550$  mm. The beam is simply supported with the span of  $l = 500$  mm (see Fig. 3), according to RILEM recommendations for fiber reinforced concrete structures TC 162-TDF [14]. The notch at the mid-length of the beam was cut 28 days after casting using the wet sawing method. The beam was turned on its side at  $90^\circ$  against the casting surface and the notch was sawn over the entire width. The notch width is 5 mm and 25 mm in length (see Fig. 3).

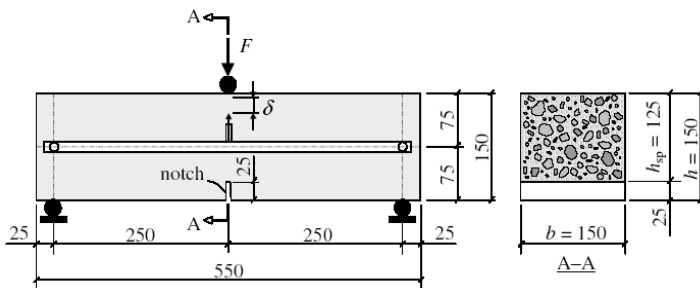
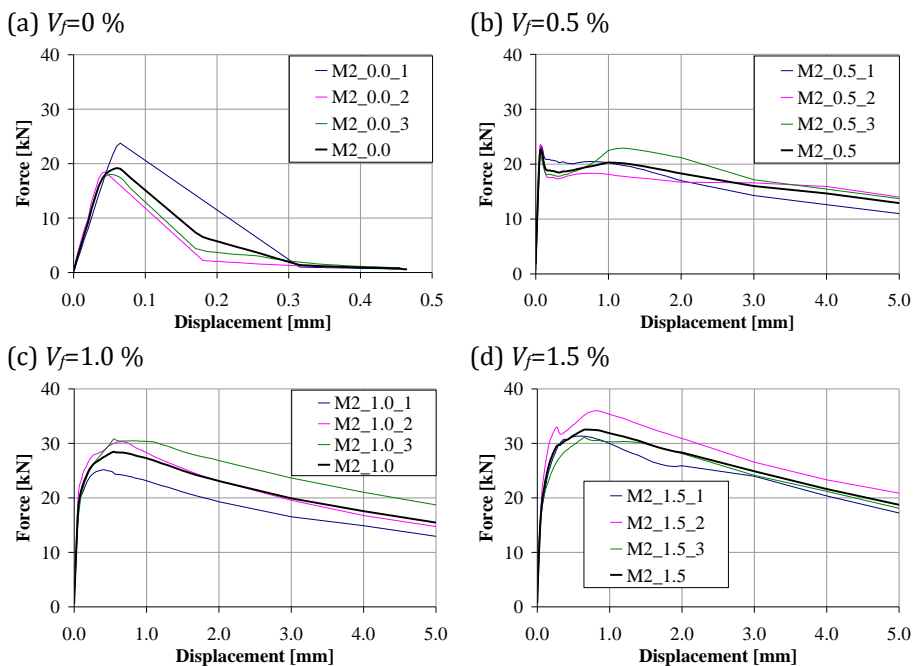


Figure 3. Pre-notched beam geometry and 3-point bending test set-up [14]

The beam is loaded by displacement control with displacement rate at the mid-span of 0.01 mm/min for plain concrete beams and 0.2 mm/min for the fiber reinforced beams, respectively. For fiber reinforced beams the displacement controlled test is carried out up to the total displacement of approximately 30 mm. During the test the load and displacement at the bottom surface of the beam were continuously measured.

The tests are performed for three different concrete mixtures, each containing four different fiber volume fractions ( $V_f = 0\%$ ,  $0.5\%$ ,  $1.0\%$  and  $1.5\%$ ) and for each fiber volume fraction three specimens are tested, i.e. in total 36 specimens are tested.

Experimentally obtained load-displacement curves for the beams cast in M2 mixture, with different fiber volume fractions ( $V_f = 0\%$ ,  $0.5\%$ ,  $1.0\%$  and  $1.5\%$ ) are plotted in Fig. 4. Each figure shows the load-displacement relationship for all tested specimens as well as the mean value of the results (black colour). For plain concrete beams ( $V_f = 0\%$ ) the displacement up to 0.5 mm is shown, while for fiber reinforced concrete ( $V_f = 0.5\%$ ,  $1.0\%$  and  $1.5\%$ ) the displacement up to 5.0 mm is plotted.



**Figure 4.** Experimentally measured load - displacement curves for beams with different fiber volume fractions of mixture M2

It can be seen that up to the formation of the first crack in concrete the load-displacement curves are almost identical for all beams and only after the first crack appearance large scatter of measured data can be observed. As expected, with addition of steel fibers the beam response becomes more ductile. It is obvious that with increasing the fiber volume fraction, the resistance and ductility of the beams increase. In all cases the failure is due to the mode-I bending with formation of single discrete crack.



### 3. Meso scale modelling approach

In the nonlinear finite element analysis [15], performed at meso scale, fiber reinforced concrete was considered as a three-phase composite consisting of concrete, fibers and the discrete interface between them. Concrete is discretized by 3D finite elements with the microplane model [16] as a constitutive law. The fibers are modelled as simple truss finite elements that are randomly distributed over the concrete and the uniaxial stress-strain relationship for steel is used as a constitutive law. The connection between concrete and fibers is simulated with discrete bond-slip relationship [17].

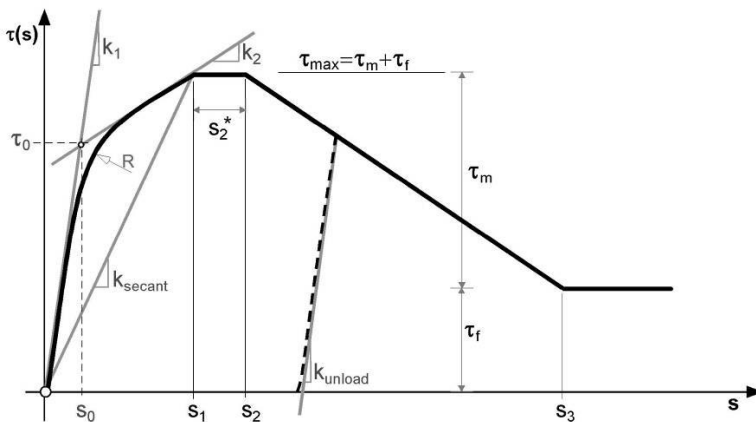


Figure 5. Discrete bond-slip relationship

In the finite element model the bond model simulates the connection between concrete 3D finite elements and the fibers that are represented by 1D truss finite elements. The connection perpendicular to the fiber orientation is assumed to be perfect and the connection in direction of fiber axis is defined by discrete bond-slip law. The fiber slip  $s$  represents a relative displacement between “the same” concrete and the fiber node in direction of fiber axis. It is modelled using zero length nonlinear spring element (Fig. 5) [17].

#### 3.1. Generation of fiber finite elements

For the defined 3D space of the beam the fibers are generated randomly. For the given length of fibers (35 mm) the position of their center of gravity and orientation are chosen as a random variables. The random generator should fulfill two basic constrains, the volume content of fibers and the distance between them should be larger than certain in advance defined threshold value. Once the fibers are generated they are discretized by four

truss finite elements. The fibers are discretized by the straight bars, i.e. the hooks are not modelled (see Fig. 6). Note that their mechanical effect is taken into account indirectly through the effective bond-slip relationship. Truss finite elements are used as a constraint for the generation of four node concrete solid finite elements. At the common points two nodes are introduced and connected with zero length nonlinear spring elements, which represent bond-slip constitutive law, as defined above.

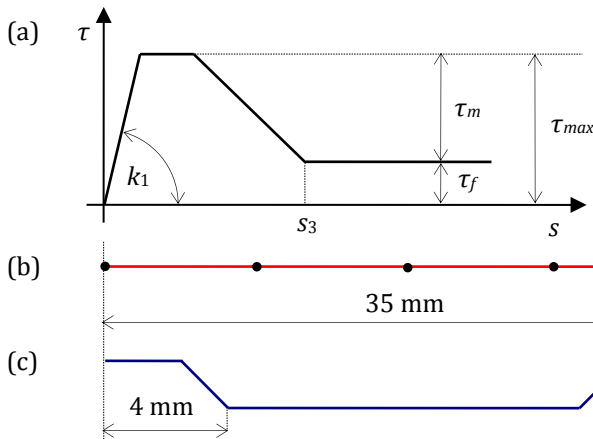


**Figure 6.** Finite element idealization of fibers: (a) bond-slip relationship, (b) four truss finite elements and (c) actual fiber shape

In order to save computational time, in the 3-point bending finite element analysis of the beam, only central part of the beam (150x150x150 mm) is modelled as a three-phase material. The rest of the beam, which is out of the zone of interest, is modelled using standard 3D solid finite elements representing fiber reinforced concrete at macro scale. Furthermore, in the analysis simplified version of the bond-slip relationship from Fig. 5 is used in most cases with the assumption  $R = \infty$  (see Fig. 6). The essential parameters for the calibration of the bond - slip relationship ( $\tau$ - $s$ ) are:  $k_1 = k_2 = k_{secant}$ ,  $\tau_{max} = \tau_m + \tau_f$  and  $s_3$ . Note that  $\tau_m$  is mechanical bond (contribution of hooks) and  $\tau_f$  is the contribution of friction to bond.

## 4. Numerical analysis

### 4.1. Finite element model

The numerical analysis is carried out only for the beams made of M2 concrete mixture with for different fiber volume fractions ( $V_f = 0\%$ ,  $0.5\%$ ,  $1.0\%$  and  $1.5\%$ ). For the finite element discretization of the beam with fiber content  $V_f = 0.5\%$  and  $V_f = 1\%$ , in total 1874 and 3784 fibers, respectively, are

generated in the middle zone of the beam. Due to the limitations of the mesh generator, the finite element mesh for the case  $V_f=1.5\%$  is the same as for the case  $V_f=1.0\%$ , however, the cross-section area and diameter of the fibers are adopted accordingly, i.e. an increase of 1.5 times in the fiber cross section area and fiber circumference are accounted for. The models for plain concrete ( $V_f=0\%$ ) are generated for concrete meshes that correspond to  $V_f=0.5\%$  and  $V_f=1.0\%$ . These two models are marked with  $V_f=0.0\%$  (0.5%) and  $V_f=0.0\%$  (1.0%), respectively. Note that the discretizations without bond elements and fibers need to be verified with respect to the mesh objectivity, i.e. two different meshes for plain concrete beams should result to the same response. The typical finite element discretizations for beams with 0.5% and 1.0% of volume fiber fractions together with random distribution of fibers are shown in Fig. 7.

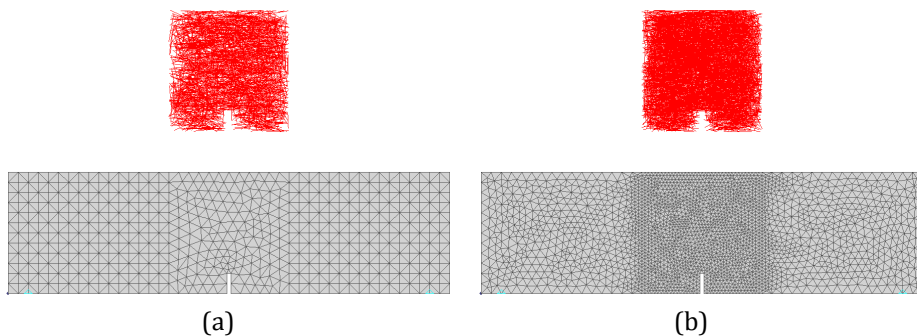


**Figure 7.** Finite element discretization of concrete and fibers for fiber volume content of 0.5% and 1.0%: (a)  $V_f=0.5\%$ , entire beam view and (b)  $V_f=1.0\%$ , entire beam view

#### 4.2. Calibration of concrete parameters

The model parameters are obtained by fitting of test results for plain concrete beams loaded in 3-point bending under displacement control. The resulting macroscopic properties of concrete are: Young's modulus  $E_c = 38652$  MPa, Poisson's ratio  $\nu_c = 0.18$ , uniaxial compressive strength  $f_c = 75.0$  MPa, uniaxial tensile strength  $f_t = 5.24$  MPa and fracture energy  $G_F = 0.092$  J/m<sup>2</sup>. In Fig. 8 are plotted experimentally and numerically obtained curves for two different meshes. As can be seen the agreement between experimental and numerical results is reasonably good for both discretizations.

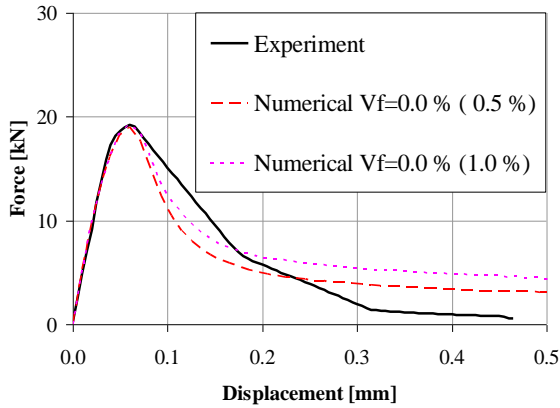


**Figure 8.** Load-displacement curves for plain concrete beam, numerical and experimental results

### 4.3. Effective bond - slip relationship of single fiber

Based on the experimentally obtained bond-slip relationship for single fiber (mean value, Fig. 2), the model parameters for the effective bond-slip curve of single fiber are obtained by minimizing the error between experimentally obtained bond-slip relationship and constitutive law shown in Fig. 5. Based on this, the discrete bond model parameters are obtained as:  $\tau_m=10.17$  MPa,  $\tau_f=1.83$  MPa,  $k_{secant}=17.129$  MPa/mm,  $k_1=41.808$  MPa/mm,  $k_2=2.707$  MPa/mm,  $s_2^*=0.2$  mm,  $s_3= 4.8$  mm and  $R=3.039$ . The comparison between the experimental bond-slip curve and the constitutive law is shown in Fig. 9a.

The influence of the bond-slip relationship on the response of the beam is first studied for the concrete mix with volume fiber fraction of 0.5%. The analysis is carried out using bond-slip constitutive law for pull-out of single fiber (case BS-P, see Table 2). The comparison with the experimental results (see Fig. 9b) shows that the peak resistance is well estimated, however, the post-peak response is too brittle. There are two reasons for this; firstly, the bond-slip relationship for a single fiber does not account for the interaction between fibers and, secondly, in the critical section of the beam fibers are loaded (pulled out) in directions that do not coincide with the their axis, i.e. there is also dowel action which leads to the increase of the stiffness of the effective bond-slip relationship.

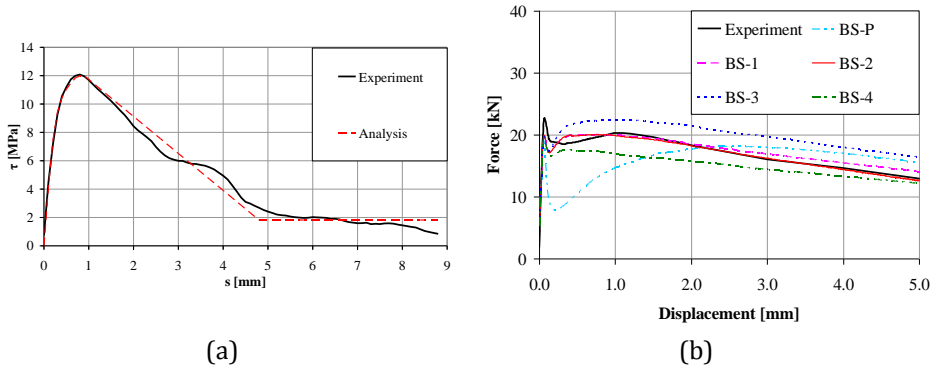


**Figure 9.** (a) Experimental bond - fiber slip relationship ( $\tau$ - $s$ ) and fit obtained from numerical analysis and (b) Comparison between experimentally and numerically obtained load - mid span displacement curves ( $V_f=0.5\%$ ) for different bond-slip relationships

**Table 2.** Discrete bond model parameters for  $V_f = 0.5\%$

| Case | Model parameters  |                   |                          |                   |                   |                 |               |      |
|------|-------------------|-------------------|--------------------------|-------------------|-------------------|-----------------|---------------|------|
|      | $\tau_m$<br>[MPa] | $\tau_f$<br>[MPa] | $k_{secant}$<br>[MPa/mm] | $k_1$<br>[MPa/mm] | $k_2$<br>[MPa/mm] | $s_2^*$<br>[mm] | $s_3$<br>[mm] | $R$  |
| BS-P | 10.17             | 1.83              | 17.13                    | 41.81             | 2.71              | 0.20            | 4.80          | 3.04 |
| BS-1 | 10.17             | 1.83              | 1200                     | 1200              | 1200              | 0.20            | 4.80          | -    |
| BS-2 | 10.17             | 1.83              | 1200                     | 1200              | 1200              | 0.20            | 4.00          | -    |
| BS-3 | 12.55             | 1.83              | 1200                     | 1200              | 1200              | 0.20            | 4.80          | -    |
| BS-4 | 7.76              | 1.83              | 1200                     | 1200              | 1200              | 0.20            | 4.80          | -    |

To obtain better fit of the experimental results a parametric study is carried out. In the study the simplified version of the bond-slip relationship (see Fig. 6a) is used in which, compared to the single bond-slip relationship, stiffness  $k_1$ ,  $k_2$  and  $k_{secant}$  are increased and all equal to 1200 MPa/mm, keeping all other parameters the same (case BS-1, see Table 2). With these parameters for bond-slip relationship the analysis shows very good agreement with the experiments almost in the entire displacement range, up to 5 mm. To further improve the response for large displacements, in the next step slip parameter  $s_3$  is slightly decreased, from 4.8 mm to 4.0 mm (case BS-2). The resulting curve obtained from the meso-scale model exhibit now excellent agreement with the experimental curve, not only for the pre-peak response and resistance but also for the entire post-peak response in the range up to displacement of 5 mm. Finally, the effect of bond strength on the response of the beam is investigated by varying peak resistance (12.0 MPa, case BS-1) in the range of  $\pm 20\%$  (cases BS-3 and BS-4). From Fig. 9b

can be seen that this leads to the positive and negative shift, respectively, of the post-peak response. Based on the comparison of the numerical and experimental data it can be concluded that the best fit for  $V_f = 0.5\%$  is obtained for the bond-slip relationship BS-2.

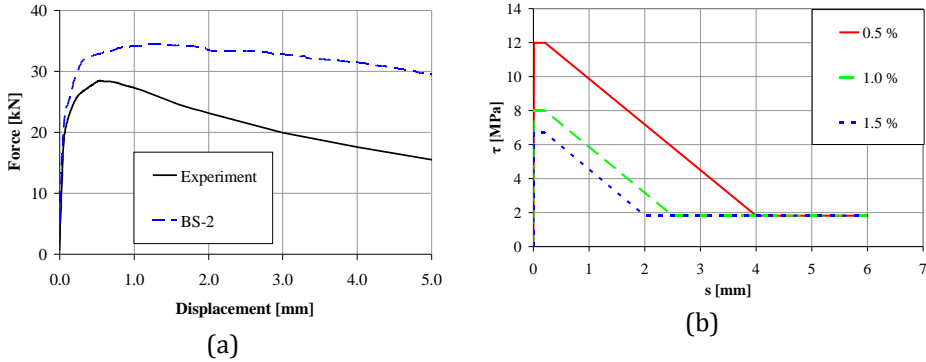


**Figure 10.** (a) Comparison between experimentally and numerically obtained load - mid span displacement curves ( $V_f=1.0\%$ ) and (b) Fiber bond - slip relationship ( $\tau$ - $s$ ) for fiber reinforced concrete beams with different fiber volume fractions

If one employs the bond-slip relationship obtained from the calibration of the model with  $V_f = 0.5\%$  for the beams with higher content of fibers then the resulting resistance is overestimated and the post-peak response too ductile. This is illustrated in Fig. 10a which shows the comparison between the corresponding experimental data and numerical simulation using bond slip relationship for the case BS-2. The reason for this is obvious, namely, due to the higher content of fibers the interaction between fibers leads to the reduction of the pull-out capacity of fibers. Therefore, it is necessary to adopt the bond-slip relationship on the volume content of fibers. This is obtained through the parametric study, similar as carried out for the fiber volume content of 0.5%. In the study the starting constitutive bond-slip relationship is the case BS-2 (see Table 2). The peak resistance  $\tau_m$  and the limit slip  $s_3$  are varied such that the analysis fit the mean load-displacement curve for the fiber volume content of 1.0% and 1.5%, respectively. The optimal parameters of the bond-slip constitutive law for all three volume contents are summarized in Table 3 and the corresponding bond-slip relationships are plotted in Fig. 10b.

**Table 3.** Discrete bond model parameters for all models

| Volume content of fibers | Model parameters |                |                       |                |              |            |
|--------------------------|------------------|----------------|-----------------------|----------------|--------------|------------|
|                          | $\tau_m$ [MPa]   | $\tau_f$ [MPa] | $k_{secant}$ [MPa/mm] | $k_1$ [MPa/mm] | $s_2^*$ [mm] | $s_3$ [mm] |
| 0.5                      | 10.17            | 1.83           | 1200                  | 1200           | 0.20         | 4.00       |
| 1.0                      | 6.17             | 1.83           | 1200                  | 1200           | 0.20         | 2.50       |
| 1.5                      | 4.89             | 1.83           | 1200                  | 1200           | 0.20         | 2.00       |

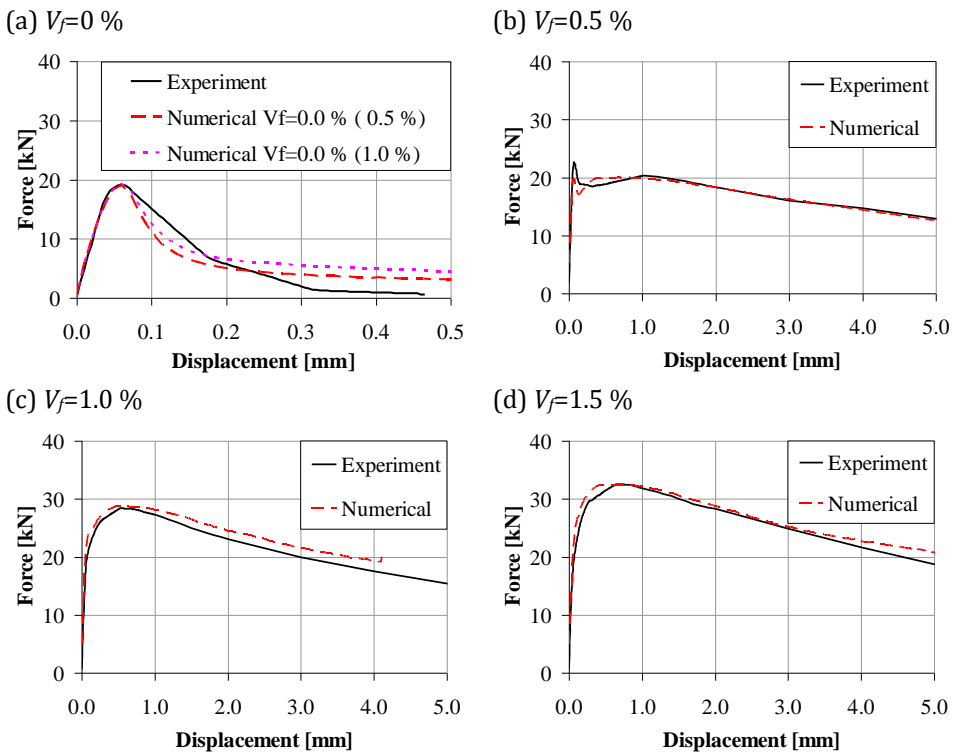


**Figure 11.** Comparison between experimentally and numerically obtained load – mid span displacement curves

The resulting load-displacement curves for the beams with volume fraction of fibers varied from 0 % to 1.5 % are shown in Fig. 11. As can be seen for the entire range of the post peak response, the agreement between numerical and experimental curves is very good. Note that for the case with 1% of fiber content the analysis was stopped at displacement of approximately 4 mm due to numerical difficulties. It can be seen that for relative low volume fraction of fibers after the peak resistance is reached

the load-displacement curve exhibit a sudden drop and subsequent recovery. This is due to the relative low volume content of fibers but is also dependent on the beam size. In case of large beams this drop would probably be even more pronounced.

In all simulations the failure is due to the bending Mode-I failure type. For the lower content of fibers damage tends to be more localized around the final discrete crack whereas for the cases with higher content of fibers damage tends to be more distributed.

## 5. CONCLUSION

Based on the results of the study, the following conclusions can be drawn out. (1) Modelling of fiber reinforced concrete at meso scale is rather demanding task since fibers, randomly oriented in space, have to be generated and connected with concrete elements using an effective bond-slip relationship. (2) It is shown that the effective bond-slip relationship cannot be obtained only from a single fiber pull-out experiments. From such a test only bond strength and maximum slip can be realistically evaluated. However, the initial stiffness is underestimated, with a consequence that the resulting pre-peak resistance is underestimated and the post-peak response is too brittle. (3) The effective bond-slip relationship is calibrated based on the fit of the experimental results for 3-point bending test data by the numerical results using bond-slip relation of a single fiber as the starting relationship. (4) The used 3D finite element analysis based on the proposed meso scale approach is able to predict pre- and post-peak behavior and peak resistance realistically. As expected, with increase of the volume fraction of fibers the resistance and ductility increases. (5) With the increase of the volume content of fibers the bond strength and maximum slip decrease. The reason is the interaction among the fibers when they come too close to each other, i.e. the local damage of concrete around fibers leads to degradation of effective bond capability. (6) The evaluation of the numerical results shows that for the investigated beams the failure is due to the failure of bond between concrete and fibers, i.e. fibers are pulled-out from the concrete. In all cases the yield stress in steel is not reached. (7) The failure is of the beams due to the mode-I bending. With increase of the volume, content of fibers local damage around discrete crack increases, which leads to the increase of ductility. (8) The proposed meso scale model is shown to be powerful numerical tool able to realistically predict behavior of fiber reinforced concrete. In combination with experimental results it can be effectively employed in design of new materials and structural elements.



## References

- [1] ACI Committee 544. State-of-the Art Report on Fiber Reinforced Concrete, ACI Manual of Concrete Practice, 2001; ACI 544.1R-96.
- [2] Kunieda M., Ogura H., Ueda N. & Nakamura H. Tensile fracture process of Strain Hardening Cementitious Composites by means of three-dimensional meso-scale analysis, *Cement & Concrete Composites*, 2011; 33: 956-965.
- [3] Han T.-S., Feenstra P.-H. & Billington S.-L. Simulation of highly ductile fiber-reinforced cement-based composite components under cyclic loading, *ACI Structural Journal*, 2003; 100(6): 749-757.
- [4] Suwada H. & Fukuyama H. Nonlinear finite element analysis on shear failure of structural elements using high performance fiber reinforced cement composite, *Journal of Advanced Concrete Technology*, 2006; 4(1): 45-57.
- [5] Fischer G., Stang H. & Dick-Nielsen L. Initiation and development of cracking in ECC materials: experimental observations and modelling, *Fracture mechanics of concrete and concrete structures FRAMCOS6*, 2007: 1517-1522.
- [6] Maalej M. Tensile properties of short fiber composites with fiber strength distribution, *Journal of Materials Science*, 2001; 36: 2203-2212.
- [7] Bolander J.E. & Saito S. Discrete modelling of short-fiber reinforcement in cementitious composites, *Advanced Cement Based Material*, 1997; 6: 76-86.
- [8] Jun P. & Mechtcherine V. Behaviour of strain-hardening cement-based composites (SHCC) under monotonic and cyclic tensile loading: Part 2 - Modelling, *Cement & Concrete Composites*, 2010; 32: 810-818.
- [9] Bolander J.E. & Sukumar N. Irregular lattice model for quasistatic crack propagation, *Physical Review B*, 2005; 71: 1-12.
- [10] Schaufert E.A. & Cusatis G. Lattice Discrete Particle Model for Fiber-Reinforced Concrete. I: Theory, *Journal of Engineering Mechanics*, 2012; 138: 826-833.
- [11] Schaufert E.A., Cusatis G., Pelessone D., O'Daniel J.L. & Baylot J.T. Lattice Discrete Particle Model for Fiber-Reinforced Concrete. II: Tensile Fracture and Multiaxial Loading Behavior, *Journal of Engineering Mechanics*, 2012; 138: 834-841.
- [12] EN 12390-3:2001 Testing hardened concrete - Part 3: Compressive strength of test specimens, 2001.

- [13] EN 12390-6:2000 Testing hardened concrete - Part 6: Tensile splitting strength of test specimens, 2000.
- [14] Vandewalle L. RILEM TC162-TDF: Test and design methods for steel fiber reinforced concrete: Bending test final Recommendation, *Materials and Structures*, 2002; 35: 579-582.
- [15] Ožbolt J. MASA – MACROscopic Space Analysis, Internal Report, Institut für Werkstoffe im Bauwesen, Universität Stuttgart, 1998.
- [16] Ožbolt J., Li Y.J. & Kožar I. Microplane Model for Concrete with Relaxed Kinematic Constraint, *International Journal of Solids and Structures*, 2001; 38: 2683-2711.
- [17] Ožbolt J., Lettow S. & Kožar I. Discrete Bond Element for 3D Finite Element Analysis of Reinforced Concrete Structures. In Balázs-Bartos-Cairns-Borosnyói (eds), *Proceedings of the 3rd International Symposium: Bond in Concrete - from research to standards*. Budapest: University of Technology and Economics, 2002.